Journal of Pharmaceutical Sciences xxx (2017) 1-8

Contents lists available at ScienceDirect

Journal of Pharmaceutical Sciences

journal homepage: www.jpharmsci.org

Pharmaceutical Nanotechnology

On-Chip Preparation of Streptokinase Entrapped in Chitosan Nanoparticles Used in Thrombolytic Therapy Potentially

Mohammad Shamsi, Payam Zahedi*

Nano-Biopolymers Research Laboratory, School of Chemical Engineering, College of Engineering, University of Tehran, PO Box: 11155-4563, Tehran, Iran

ARTICLE INFO

Article history:
Received 13 April 2017
Revised 22 June 2017
Accepted 4 August 2017

Keywords:
microfluidics
chitosan
nanoparticles
protein delivery
blood flow

ABSTRACT

The objective of this work was to prepare the streptokinase (SK) entrapped in chitosan nanoparticles (CS NPs) using bulk mixing (BM) and microfluidic (MF) techniques. The physicochemical properties of the samples were characterized by means of scanning electron microscopy and dynamic light scattering analysis for optimizing CS and SK solution concentrations as well as pH values. The obtained results showed that CS NPs fabricated using MF chip have the most uniform morphology, spherical shape, and average diameter of 67 ± 13 nm along with a narrow polydispersity. Conversely, the NP samples prepared via BM method have an irregular and disordered morphology as well as a broad distribution in their particle size (452 ± 300 nm). The *in vitro* drug release from microfluidically generated CS NPs depicted the controlled release of SK without plateau regime compared to those samples prepared using BM method during 48 h. Also, the drug release kinetic followed Higuchi model which revealed that the Fickian diffusion was the predominant mechanism. Subsequently, in *in vivo* animal model test, the performance of SK in blood plasma exhibited higher amidolytic activity for SK entrapped in CS NP samples fabricated via MF technique compared to those NPs prepared using BM and also SK alone.

Introduction

Nowadays, one of the major causes of human mortality worldwide is the bloodstream infection owing to clot formation. This disorder in its severe level leads to the stoppage of blood flow in heart, brain, and lung that results in a serious damage to these vital organs and pulmonary embolism. Although the preliminary preventions are the best solution for reducing the thrombolysis disease, the prescription of fibrinolytic drugs such as tissue plasminogen activator (tPA), streptokinase (SK), and urokinase (UK) due to their indispensable role in this way is highly recommended.

Generally, these chemical drugs are able to convert plasminogen to plasmin as a natural fibrinolytic agent in the blood plasma, thereby breaking the fibrinogen and fibrin structures for thrombolysis therapy.[1-4] Amid these drugs, SK is known as the most considerable protein-based drug which enables to change plasminogen to plasmin for preventing the blood clot and embolism. SK with molecular weight of 47 kDa is a β-hemolytic extracellular and nonenzymatic protein that is widely used for thromboembolic disorders in human. It includes 414 α-amino acids without any disulfide bridges and has dielectric point at pH 4.7 that leads to plasminogen activation through a fibrinolytic process indirectly.[5] In regard to SK performance in blood plasma, it forms a complex with plasminogen immediately, leading to provide plasmin as a proteolytic factor. Subsequently, the formed plasmin can degrade the insoluble fibrin polymers and break them into different fragments in predetermined levels, as a result dissolving and disappearing them in the blood fluid stream. On the other hand, SK has a bacterial resource which is known as an antigenic reagent for immunologic system in the body. This property provides a series of antibodies in the blood plasma that extremely tend to attack the SK molecules and then obviate them immediately. This reaction is considered as the main shortcoming of SK performance, and in consequence its biological half-life is reduced in exposure to the physiological environments. Therefore, by decreasing the effective dose of SK in blood circulation, its readministration at time periods of 12 to 72 h is essential in order to keep the amount of the drug at the appropriate therapeutic level. This issue results in a series of adverse side effects for the patients.[6]

Due to rapid degradation of SK in the blood plasma, its role in thrombolysis therapy significantly decreases. To overcome this problem, many solutions have been investigated to change the molecular structure of SK including genetic mutant and chemical as

* *Correspondence to:* Payam Zahedi (Telephone: +98-(21)-61112247, 61113062; Fax: +98-(21)-66957784).
E-mail address: phdzahedi@ut.ac.ir (P. Zahedi).

http://dx.doi.org/10.1016/j.xphs.2017.08.001
0022-3549/

well as enzymatic modifications.[6-10] Among them, some polymeric carriers have also been prepared and employed to increase the SK resistance against degradation. Rajagopalan et al.[11] prepared macromolecules to maintain their performance in *in vivo* experiments using PEGylation of SK owing to postponing degradation of this protein-based drug. Moreover, by using liposomes, these materials have shown a great potential as carriers for improvement of SK half-life.[12,13] In another study, Leach et al.[14] compared the thrombolysis potential of the prepared samples based on pure SK, SK encapsulated into liposome, and SK microencapsulated into poly(ethylene glycol) (PEG) on rabbit animal models. They revealed that the samples based on PEG showed the highest reperfusion compared with another 2 samples. The main disadvantage of these nanocarriers was the conventional method used for their production. It is worth noting that the bulk mixing (BM) as a common method leads to provide nanoparticles (NPs) with nonuniform distribution in their size and irregular morphology. This method results in a series of unrepeatable outcomes for each batch. In contrast to liposomes and PEG, chitosan (CS) chains are able to provide a strong electrostatic interaction with thrombolytic drug molecules. Recently, Chen et al.[15] studied the magnetically controlled release of recombinant tPA from CS nanocomposites for targeted thrombolysis. They showed that the ionic cross-linking of water-soluble CS in the presence of recombinant tissue plasminogen activator (rtPA) and magnetite (Fe_3O_4) NPs could produce rtPA-encapsulated magnetic CS NPs. These samples had negligible rtPA protein release when stored in phosphate buffer for 28 days; in contrast, the burst release of rtPA from the CS NPs found in the serum was 60% of the original activity released in 30 min.

However, it is predicted that using microfluidic (MF) technique owing to its unique process characteristics can enhance the physicochemical properties of CS NPs for protein delivery.

In the past few years, employing biopolymer-based NPs with an emphasis on CS as drug carriers has received a great deal of interest.[16,17] CS is an N-deacetylated derivative of chitin that can be obtained from crustacean exoskeletons or via fungal fermentation processes. CS has been widely used in biomedical and drug delivery applications owing to its unique properties such as biodegradability, nontoxicity, biological inert effect, good adherence to peptide and proteins, antitumor and antibacterial activities as well as blood hemostasis. Furthermore, this polysaccharide is relatively cheap and available.[18,19] CS can provide a good complex with drugs especially proteins which have opposite charges against CS, and hence this polymer has high entrapment capability of those drug molecules to achieve an efficient drug delivery system.[20-24] The entrapment efficiency (EE) of drug in a polymeric carrier depends on a series of different parameters such as preparation methods of NPs, physicochemical characteristics of drug, drug-polymer interactions, and also nature of other added ingredients.[25-27] The scientists in their recent works have clearly shown that the microfluidically fabricated NPs based on synthetic and natural biopolymers like poly(lactic-co-glycolic) acid and CS have a high capacity value for drug loading.[28,29] In addition, the protein drug loading into CS NPs prepared using MF chips not only increases the entrapment efficacy, but this technique also leads to the formation of those NPs with a uniform shape, small size, and narrow polydispersity.[30] It is worth noting that many reports have been published on CS NPs containing SK by the use of traditional BM method.[31-33] Nevertheless, there is a lack of effort on this drug-polymer system based on MF as a promising bottom-up precipitation technique.

This work is aimed at preparing CS-based NPs containing SK by using both MF and BM methods in order to compare them. Then, the physicochemical properties of the samples such as morphology, drug EE, and its release are investigated. Subsequently, the *in vitro* release kinetic of SK entrapped in those NPs are discussed in detail based on different models. Finally, an *in vivo* animal model experiment is operated for assessing the activity of SK entrapped in CS NPs in blood plasma.

Materials and Methods

Materials

CS (low molecular weight of 60-120 kDa) and bovine serum albumin were purchased from Sigma-Aldrich (St. Louis, MO). SK was supplied from Boehringer Company (Mannheim, Germany). The plasmin-specific substrate (s-2251) was provided from Chromogenix, Germany. The other chemicals as analytical reagent grades were obtained from Merck Company (Darmstadt, Germany), and used without further purification.

Preparation of CS-Based NP Samples Containing SK

Figures 1a and 1b show the overall schematic representation of SK entrapped in CS NPs by means of MF and BM methods, respectively. Accordingly, weighed CS powder was added to acetic acid solution (1% [v/v], pH 5) and stirred at room temperature for 2 h to produce solutions with concentrations of 1-5 mg/mL. Also, weighed SK powder was diluted in distilled water with concentrations of 0.1-2 mg/mL. In regard to BM method, the diluted drug was added dropwise to different CS solutions while stirring (300 rpm) at temperature of 4°C until the mixture with entrapped drug was attained (Fig. 1b). This process was carried out for 60 min and the prepared SK entrapped in CS NPs were denoted by BMCSSK. As is shown in Figure 1a for MF technique, the programmable syringe pumps injected separately the CS solutions from lateral channels followed by the SK solution inserted into the central channel with the shape of T-junction embedded in the MF chip. The solution concentrations were the same as those mentioned earlier for producing NPs based on BM. The CS-to-SK flow rate ratios (Q_{CS}/Q_{SK}) were adjusted at 0.5, 1, and 2 for the formation of hydrodynamic flow focusing phenomenon through the cross-section region. Eventually, the resulting NP suspensions exited from the MF chip were collected and denoted by MFCSSK0.5, MFCSSK1, and MFCSSK2 (Table 1).

Characterization of CS NPs Containing SK

EE of SK in CS NPs

For calculating the EE of SK (EESK) in CS-based NPs prepared by both BM and MF processes, they were centrifuged with a speed of 18,000 rpm at 4°C for 20 min and then the powder samples were attained using a laboratory freeze dryer (Alpha 1-2/LD Plus; Martin Christ, Osterode am Harz, Germany). The amounts of SK in the supernatants were evaluated by using Bradford[34] protein assay. In this procedure, bovine serum albumin and CS solutions were applied as standard and blank samples, respectively. The EESK values were calculated according to Equation 1:

$$\text{EESK} = \frac{\text{Total amount of SK} - \text{Free amount of SK in supernatant}}{\text{Total amount of SK}} \quad (1)$$

Morphology and Surface Charge of CS NPs Studies

The morphology and size of the resultant NPs were investigated by using a scanning electron microscopy (SEM; Philips XL30; Eindhoven, the Netherlands). Also, the average diameters of the

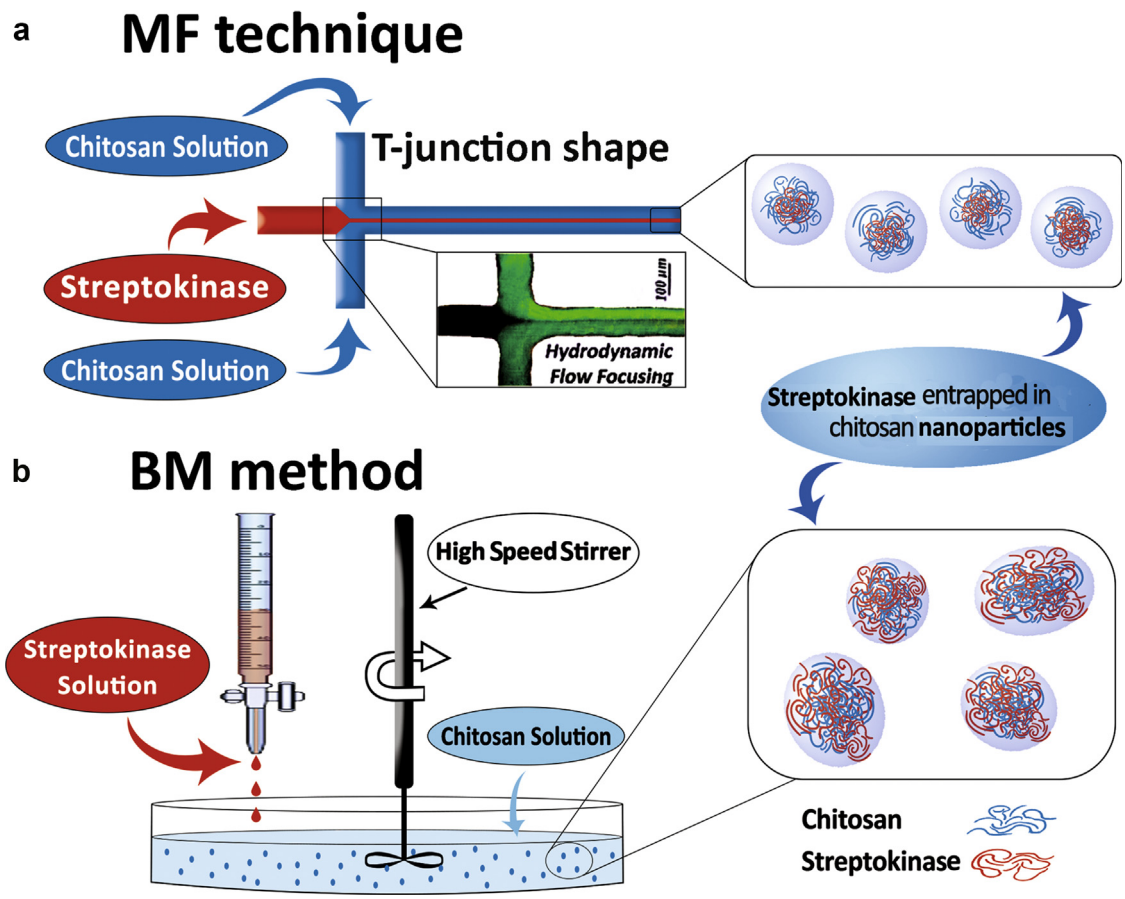

Figure 1. Schematic representation of SK entrapped in NPs based on CS by the use of (a) MF technique along with hydrodynamic flow focusing and (b) BM method.

NPs were estimated using ImageJ software and calculated by measuring about 10 different NPs for minimizing the statistical errors. The size distribution and the surface charge of the BM- and MF-based samples were measured using a dynamic light scattering (DLS) associated with a zeta-potential analyzer (Brookhaven Instruments Corporation).

In Vitro *SK Release From CS-Based NPs*

To study the SK release from the CS NPs produced using BM and MF methods, they were immersed into phosphate buffer saline (PBS, pH 7.4) at 37°C in a total volume of 10 mL. After predetermined time intervals, the NPs were collected from the suspension by using centrifugation at 16,000 rpm for 5 min and then they were suspended again in fresh PBS and the free amount of SK in the supernatant was calculated based on Bradford method mentioned earlier; the absorbance peak at wavelength of 405 nm was read by means of an ultraviolet-visible spectrophotometry (Termo 2000; Nanodrop software). The SK release at each point was recorded, and the drug calibration curve with the regression coefficient of 0.9991 (R^2) was obtained according to Beer-Lambert law (Eq. 2):

$$A = 0.86 \times c \tag{2}$$

where "A" and "c" are the drug solution absorbance and concentration, respectively. After that, the cumulative release of SK was calculated based on Equation 3 as follows:

$$\text{Cumulative release percentage}(\%) = \frac{\sum_{t=0}^{t} M_t}{M_0} \tag{3}$$

where "M_t" is the amount of released SK from the NPs and "M_0" is the total amount of SK in the NPs.

Table 1
The Recipes of Different Conditions for Fabricating the SK Entrapped in CS NPs by the Use of BM and MF Methods

Sample	Preparation Method	CS Flow Rate (mL/h)	SK Flow Rate (mL/h)	Flow Rate Ratio
BMCSSK	BM	ND	ND	ND
MFCSSK0.5	MF	5	10	0.5
MFCSSK1	MF	5	5	1
MFCSSK2	MF	10	5	2

ND, not determined.

Release Kinetic Model Analysis of SK Entrapped in CS NPs

To investigate the release profiles of BMCSSK and MFCSSK, the drug-release kinetic was also studied by the use of 5 well-known models including zero-order, first-order, Higuchi, Hixon-Crowell, and Korsmeyer-Peppas.[35,36] These models can explain how drug molecules can move from inner layers of a polymeric carrier to its surface and release into an aqueous environment, which occurs by 2 main mechanisms: (1) drug diffuses out a polymer matrix and (2) drug releases owing to the degradation of a polymer matrix. Equations 4-8 show the models where "Q_t" is the amount of drug dissolved at time "t," "Q_0" is the initial amount of drug in the solution (often $Q_0 = 0$), and "K" is the release constant. In Korsmeyer-Peppas equation, "M_t" and "M_∞" are the cumulative amount of drug released at time "t" and the initial drug loading, respectively. Also, "n" is the diffusion exponent suggesting the nature of the drug-release mechanism.

$$\text{Zero} - \text{order: } Q_t = Q_0 + K_0 t \quad (4)$$

$$\text{First} - \text{order: } \text{Ln}Q_t = \text{Ln}Q_0 + K_1 t \quad (5)$$

$$\text{Higuchi: } Q_t = K_H \sqrt{t} \quad (6)$$

$$\text{Hixon} - \text{Crowell: } Q_0^{\frac{1}{3}} - Q_t^{\frac{1}{3}} = K_{HC} t \quad (7)$$

$$\text{Korsmeyer} - \text{Peppas: } \frac{M_t}{M_\infty} = K_k t^n \quad (8)$$

In Vivo *Bioavailability of SK Entrapped in CS NPs*

In this work, all the experiments based on animal model were carried out according to the animal care and ethical considerations defined by a committee associated with Pharmaceutical Sciences Research Center at Tehran University of Medical Sciences. A series of male Wistar rats ($n = 4$, 250-300 g) were selected to investigate the biological stability and activity of SK through blood plasma, and the rats were divided into 4 groups as follows: group 1, those rats that received the neat CS NPs (as negative control); group 2, those rats that received CS NPs containing SK fabricated by using MF technique (MFCSSK); group 3, those rats that gained CS NPs consisting of SK prepared using BM method (BMCSSK); and group 4, those rats treated directly with SK alone (as positive control). In brief, at first, the rats were anesthetized by using a mixture of ketamine (40 mg/kg) and xylazine (15 mg/kg) and then polyethylene catheters were connected to their jugular veins in order to collect the blood samples at predetermined time intervals. After the rats were recovered, the samples were injected to their bodies by means of the tube connections. The SK concentration of all samples was adjusted to 15,000 IU/mL which was injected to the blood circulation of each rat and then these 4 groups were maintained in the cages with enough food and water. To prevent the blood clotting, sodium citrate with a concentration of 130 M and a ratio of 9:1 (blood/sodium citrate) was added to a series of sterilized microtubes . Subsequently, the blood samples were immediately centrifuged to remove their plasma and then they were kept at −20°C. The performance of SK was measured based on amidolytic activity by the formation of plasminogen-SK complex. Briefly, at first, 50 μL of each plasma sample was transferred to a 96-well plate and then 25 μL of common fresh human plasma was added to each well. After incubating the samples at 37°C for 20 min, 50 μL of S-2251 solution (0.75 mM) was added to the mixture and they were incubated again with the same conditions mentioned earlier. To suppress the procedure, 25 μL of acetic acid (10%) was added to each plate. The SK activity in blood plasma was measured by using an ELISA reader (Multiscan EX; Thermo Electron Corporation) at a wavelength of

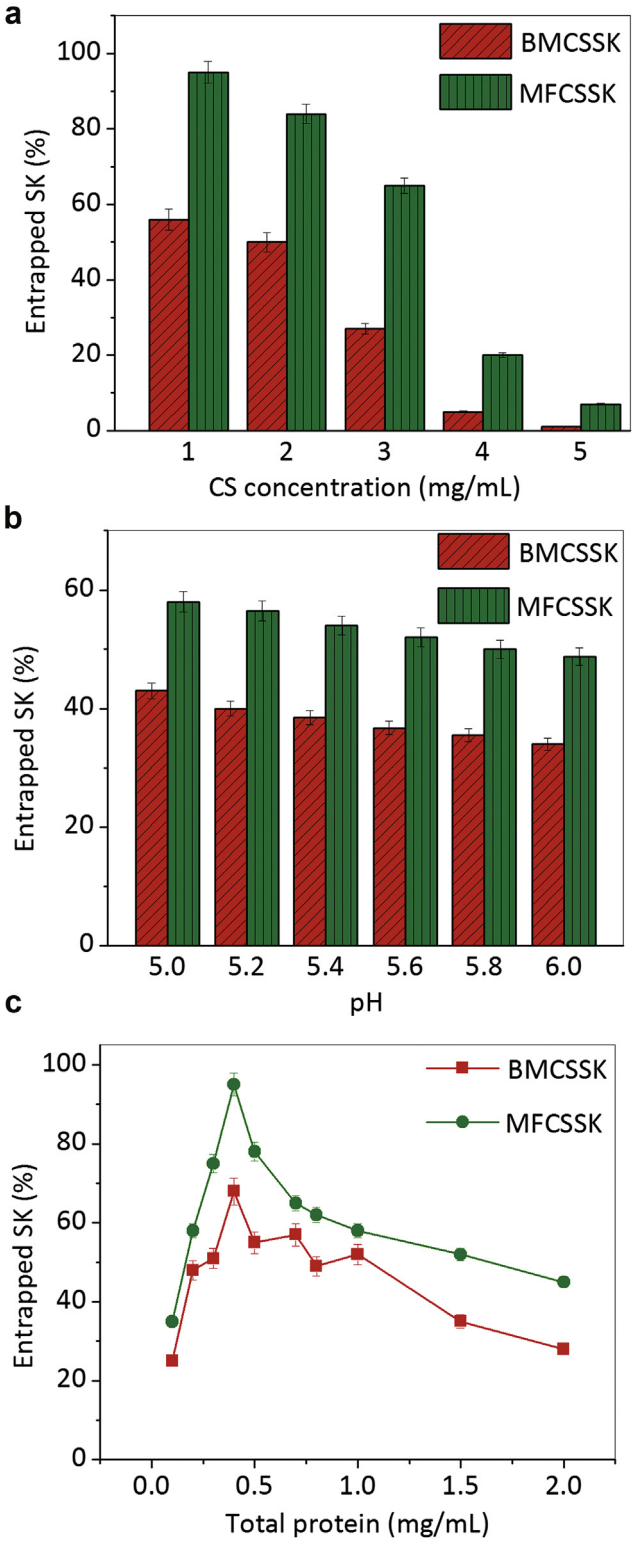

Figure 2. The effect of different parameters on EESK in CS-based NPs prepared using MF and BM methods: (a) the effect of CS concentrations, (b) the influence of pH values, and (c) the impact of total protein concentrations.

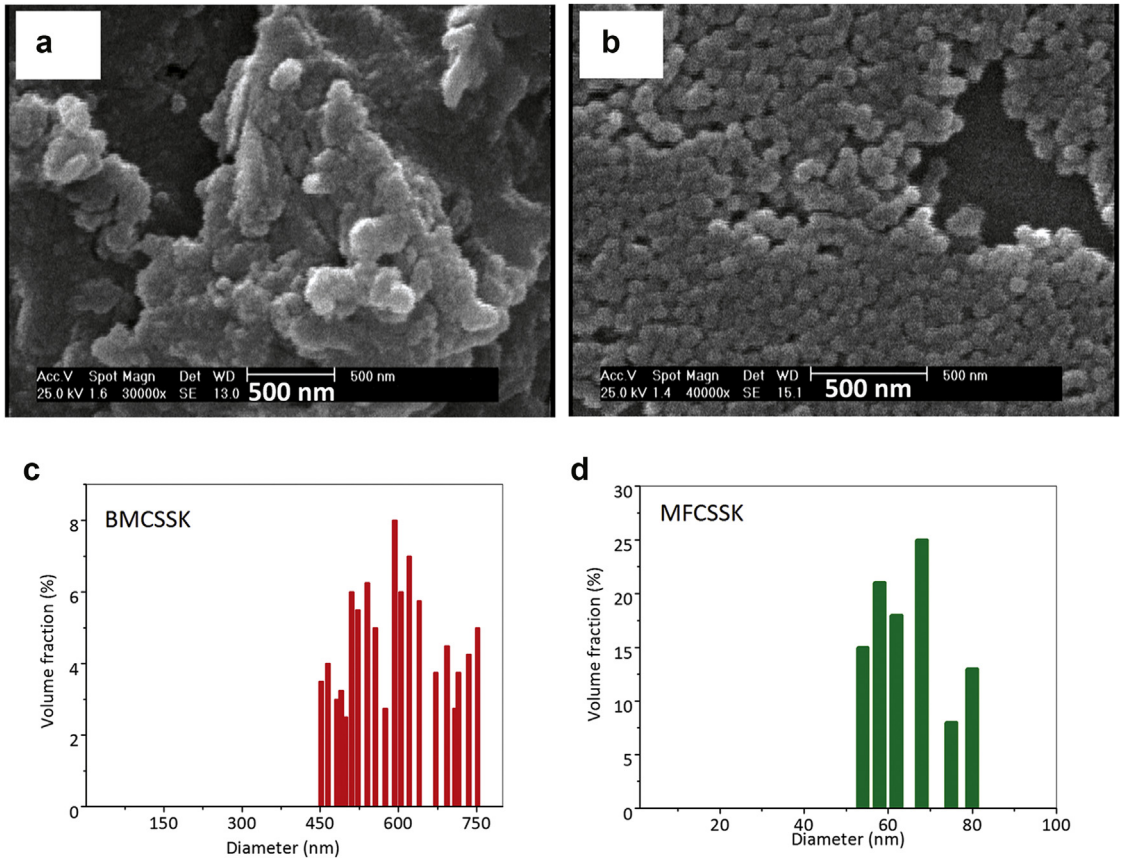

Figure 3. The SEM micrographs of SK entrapped in CS NPs produced using (a) BM method and (b) MF technique and their corresponding results obtained from DLS (c) and (d) at the optimal conditions (CS concentration of 1 mg/mL, solution pH of 5, and total protein concentration of 0.4 mg/mL).

405 nm. This test was repeated 3 times and the obtained results reported with *p* value less than 5%. It is worth noting that the SK activity determination in blood plasma was carried out based on the standard curve of this drug in the literature.[34]

Results and Discussion

Formation of Hydrodynamic Flow Focusing Through the MF Chip

The fabrication process of MF device with T-junction pattern was explained in the previous article in detail.[37] To provide CS-based NPs with controlled physical properties such as suitable compactness, small size, and narrow polydispersity, the assessment of a unique phenomenon in MF technique, the so-called hydrodynamic flow focusing, was performed. Figure 1a shows the production of MFCSSK2 using 2 colored markers, rhodamine B and sodium fluorescein. In fact, the advantage of MF technique compared to BM method is the presence of laminar flow of solutions besides hydrodynamic flow focusing, leading to CS NPs with too small size and narrow polydispersity.

The Effects of Different Parameters on EESK in CS-Based NPs and Their Morphology

Figures 2a-2c illustrate the EESK in the CS NPs as a function of different CS concentrations (1-5 mg/mL), various pH values (pH 5-6), and total protein concentrations (0.1-2 mg/mL). Commonly, medium concentrations of CS (1-3 mg/mL) in MF technique resulted in the NP formation whereas CS concentrations out of these ranges might provide a series of problems.[29] As seen from Figure 2a, the maximum EESK with amounts of 55% and 94% were obtained at 1 mg/mL of CS concentration with regard to BM and MF methods, respectively. It is worth noting that by increasing the CS concentration up to 5 mg/mL, the EESK decreased and tended to zero value with a linear behavior for those NPs prepared by using BM method. Conversely, the EESK for CS NP samples fabricated via MF technique remained at about 7%. The hydrodynamic flow focusing phenomenon in MF technique increased EESK compared to BM method. By increasing the CS concentration from 1 to 5 mg/mL, the high viscosity of CS solution restricted the entrapment of SK in CS NPs. Eventually, the CS solution with concentration of 1 mg/mL was selected as the optimum value for further evaluations. With the isoelectric points of CS and SK being 6.3 and 4.7, respectively, the effect of pH variation of the solutions on EESK was studied and it ranged from 5 to 6, which is represented in Figure 2b. As is evident, by increasing the pH, the EESK for CS NPs was decreased and also in overall, the EESK amounts of microfluidically generated CS NPs were higher than those of samples based on BM method throughout pH changes. Afterward, the EESK in CS NPs prepared by using BM and MF methods was studied as a function of total protein concentrations. As is observed from Figure 2c, at optimal total protein concentration of 0.4 mg/mL, the highest value for EESK was attained. Also, at lower and higher concentrations, a remarkable decrease in the drug entrapment occurred. This trend could be related to the monolayered adsorption phenomenon for protein-biomaterial based on the principle of Langmuir isotherm which has been first defined by Langmuir and Blodgett.[38] In conclusion, the optimum conditions for CS NP samples were as follows: CS

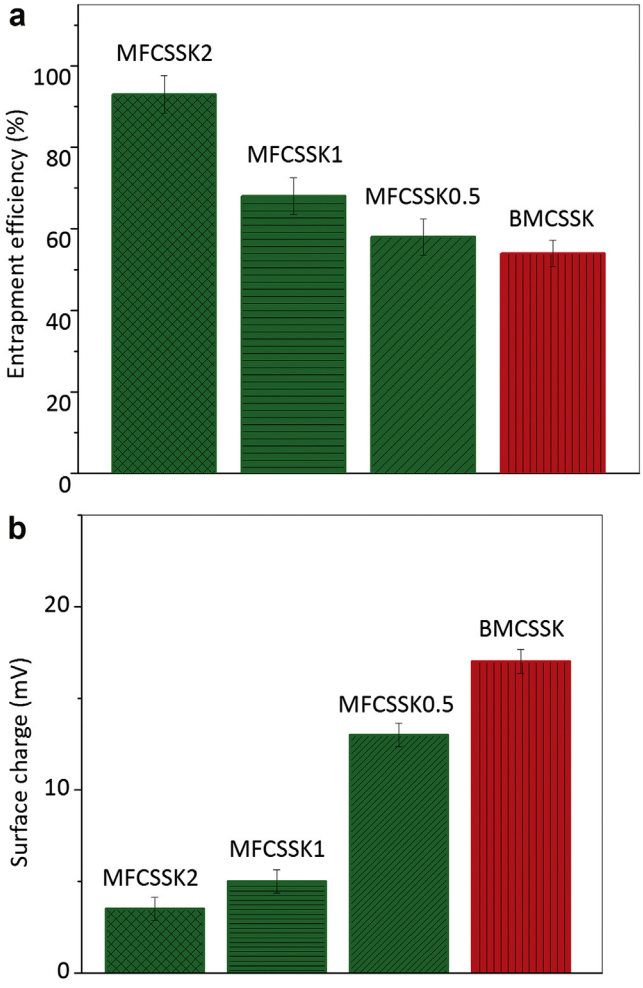

Figure 4. (a) EESK and (b) surface charge of the CS NP samples denoted by MFCSSK0.5, MFCSSK1, MFCSSK2, and BMCSSK at the optimal conditions (CS concentration of 1 mg/mL, solution pH of 5, and total protein concentration of 0.4 mg/mL).

concentration of 1 mg/mL, solution pH of 5, and total protein concentration of 0.4 mg/mL.

Figures 3a-3d depict the SEM micrographs and DLS data of BMCSSK and MFCSSK2 samples according to the optimized conditions. The obtained results from SEM and DLS clearly revealed that the MFCSSK2 samples have a uniform morphology containing NPs with a spherical shape and their average size was estimated as small as 67 ± 13 nm (Figs. 3b and 3d). In contrast to MFCSSK2, the BMCSSK samples have particles with irregular and nonspherical shape, and their average size was in submicrometers of about 452 ± 300 nm (Figs. 3a and 3c). The other samples including MFCSSK0.5 and MFCSSK1 also have the average diameter sizes of 106 ± 23 and 84 ± 17 nm, respectively. Amid the samples prepared using MF technique, MFCSSK2 due to higher compactness was selected for further evaluation.[28-30] On the other hand, Figures 4a and 4b demonstrate EESK in BMCSSK and MFCSSK samples along with their surface charge changes. As is seen, by increasing the Q_{CS}/Q_{SK} from 0.5 to 2 for MFCSSK samples, the EESK increased from 55% to 94%, whereas the surface charge decreased from 13 to 3 mV. The reason of this trend could be due to increasing the electrostatic interactions between the positive and negative portions of CS and SK in a microscale level. As the BM method works at the centimeter scale and has difficulty in providing homogenous reaction conditions, only lower amounts of SK molecules were entrapped in

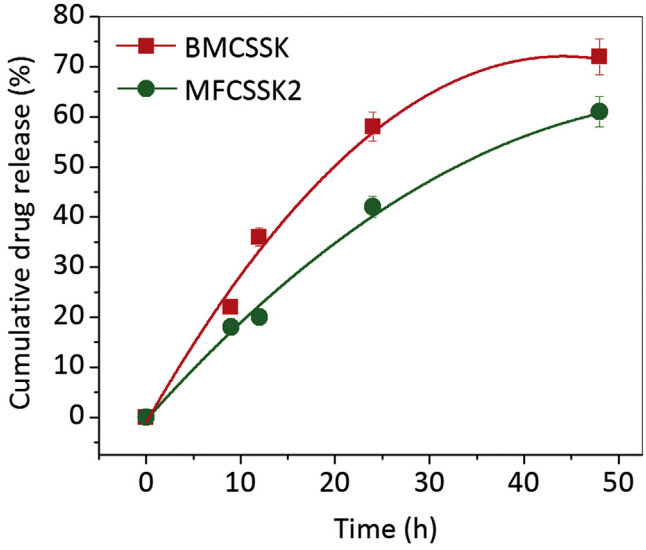

Figure 5. The cumulative SK release of BMCSSK and MFCSSK2 samples during 48 h at the optimal conditions (CS concentration of 1 mg/mL, solution pH of 5, and total protein concentration of 0.4 mg/mL).

BMCSSK (~54%), thereby obtaining higher surface charge (~17 mV). It could be concluded that in the MF technique compared to BM method, higher amounts of SK molecules were adsorbed through CS NP layers which led to a reduction in positive surface charge of MFCSSK samples.

In Vitro *SK Release From BMCSSK and MFCSSK2 Along With Their Release Kinetic Model Studies*

Figure 5 shows the SK release profiles of BMCSSK and MFCSSK2 in PBS (pH 7.4) at a physiological release environment during 48 h. As is seen, the rate of SK release from the MFCSSK2 samples was slower than that of BMCSSK along with a gentle slope in the profile. Moreover, the drug release behavior of BMCSSK samples reached a plateau state after about 30 h, which meant that after this time until 48 h there were no drug molecules to diffuse from the sample to the PBS. Interestingly, the SK release from the MFCSSK2 samples continued gradually throughout the release time and even after that. This was due to a series of unique MFCSSK2 properties in terms of high EESK, uniformity, and compactness of NPs with the spherical shape that was provided by the MF method. Furthermore, the SK release kinetic of the samples was investigated by using the well-known Korsmeyer-Peppas equation by which the main mechanism of SK release from the samples was governed by Fickian diffusion theory. This conclusion arose because the "n" value in this equation was kept at 0.5 after experimental data fitting. Table 2 represents the regression coefficients of 4 more models such as zero-order, first-order, Higuchi, and Hixon-Crowell for the SK release from the samples, and the best fitting was obtained from Higuchi model with the highest regression coefficient of 0.97 and 0.88 for the BMCSSK and MFCSSK2, respectively, which confirmed

Table 2
Regression Coefficients of Different Mathematical Models Fitted to the Release of SK From BMCSSK and MFCSSK2 With Concentration of 300 μg/mL (Mean ± SD, $N = 3$)

Sample	Zero-Order	First-Order	Higuchi	Hixon-Crowell
BMCSSK	0.8 ± 0.05	0.84 ± 0.06	0.97 ± 0.07	0.86 ± 0.02
MFCSSK2	0.64 ± 0.06	0.52 ± 0.07	0.88 ± 0.03	0.45 ± 0.05

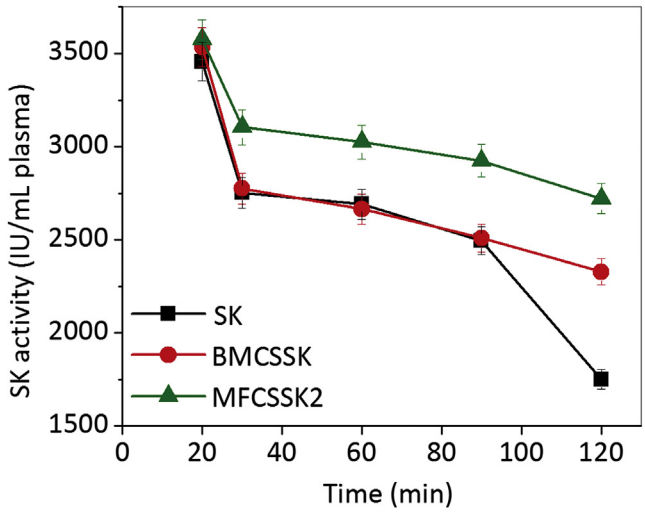

Figure 6. The SK activity trend in blood plasma during 2 h for samples containing MFCSSK2, BMCSSK, and SK alone at the optimal conditions (CS concentration of 1 mg/mL, solution pH of 5, and total protein concentration of 0.4 mg/mL).

that the drug molecule penetration followed the diffusion phenomenon.

In Vivo *SK Activity Studies in the Blood Plasma*

As mentioned earlier, in this assay, 4 different samples including neat CS NPs, MFCSSK2, BMCSSK, and also the drug alone were injected into the vein of each group of rats. It should be noted that the SK concentration in the samples containing SK and SK alone was the same and was equal to 300 μg/mL. Figure 6 demonstrates the variations in SK activity in blood plasma against the post-treatment time (2 h). Regarding SK used directly, a significant decrease in SK activity was noted in the environment especially after 90 min. In other words, pure SK without CS coating does not have enough stability in the blood plasma because of its short half-life. As a result of this trend, this drug could not act efficiently for long-term thrombolytic therapy unless a periodical administration of the drug was prescribed. In contrast, a different trend was observed for SK activity for the drug entrapped in CS NPs. A decline in SK activity in blood plasma for BMCSSK and MFCSSK2 was mainly due to the level of incorporation of drug molecules into the CS NPs. As is shown in Figures 1a and 1b, the SK molecules were completely put in the MFCSSK2 layers whereas this did not happen for BMCSSK. In other words, the multilayered MFCSSK2 could protect the drug molecules against different immunologic reagents like macrophages present in the blood plasma. Therefore, not only could SK molecules be released gradually into the plasma, but also their degradation could be postponed. On the other hand, the neat CS NPs have no drug, which in turn indicates that the level of SK activity in the blood plasma was zero. Hence, there were no data to be reported for these samples. Eventually, by comparing the SK activity results in blood plasma obtained from SK used directly, BMCSSK, and MFCSSK2, a reduction of 50%, 34%, and 28% was observed, respectively, after 2 h.

Conclusions

In this work, we showed that the CS NPs fabricated using MF technique were promising nanocarriers for increasing the half-life and entrapment capacity of SK. These unique properties could easily be attained by controlling a series of main parameters such as CS and SK concentrations, their flow rate ratios, pH values, and total protein concentrations through MF chip. The optimized conditions with which SK entrapped in CS NPs with uniform spherical shape and average diameter size of 67 ± 13 nm could be prepared were as follows: CS concentration of 1 mg/mL, SK concentration of 0.4 mg/mL, Q_{CS}/Q_{SK} of 2, and pH of 5. Accordingly, the EESK in MFCSSK2 was higher compared with the other samples, especially BMCSSK. The appropriate characteristics of MFCSSK2 samples such as their high uniformity in morphology and compactness led to a sustained, controlled release of SK drug in PBS and the release mechanism followed Higuchi model. Finally, the SK activity of MFCSSK2 in blood plasma revealed remarkable performance compared to other samples in *in vivo* animal model test and exhibited good potential in the treatment of thrombolytic disorder.

Acknowledgments

The authors would like to acknowledge the financial support of University of Tehran Science and Technology Park for this research under grant number 94057.

References

1. Banerjee A, Chisti Y, Banerjee UC. Streptokinase—a clinically useful thrombolytic agent. *Biotechnol Adv*. 2004;22(4):287-307.
2. Baruah DB, Dash RN, Chaudhari MR, Kadam SS. Plasminogen activators: a comparison. *Vascul Pharmacol*. 2006;44(1):1-9.
3. Craig CR, Stitzel RE. *Modern Pharmacology With Clinical Applications*. 6th ed. Philadelphia, PA: Lippincott Williams & Wilkins; 2004.
4. Marshall RS. Progress in intravenous thrombolytic therapy for acute stroke. *JAMA Neurol*. 2015;72(8):928-934.
5. Brockway WJ, Castellino FJ. Characterization of native streptokinase and altered streptokinase isolated from a human plasminogen activator complex. *Biochemistry*. 1974;13(10):2063-2070.
6. Wu XC, Ye R, Duan Y, Wong SL. Engineering of plasmin-resistant forms of streptokinase and their production in Bacillus subtilis: streptokinase with longer functional half-life. *Appl Environ Microbiol*. 1998;64(3):824-829.
7. Chapurina YE, Drozdov AS, Popov I, Vinogradov VV, Dudanov IP, Vinogradov VV. Streptokinase@ alumina nanoparticles as a promising thrombolytic colloid with prolonged action. *J Mater Chem B*. 2016;4(35):5921-5928.
8. Nguyen HX, Edgar AO. An in vitro thrombolysis study using a mixture of fast-acting and slower release microspheres. *Pharm Res*. 2016;33(7):1552-1563.
9. Shi GY, Chang BI, Su SW, et al. Preparation of a novel streptokinase mutant with improved stability. *Thromb Haemost*. 1998;79(5):992-997.
10. Torréns I, Ojalvo AG, Seralena A, Pupo E, Lugo V, Páez R. A mutant streptokinase lacking the C-terminal 42 amino acids is less reactive with preexisting antibodies in patient sera. *Biochem Biophys Res Commun*. 1999;266(1):230-236.
11. Rajagopalan S, Gonias SL, Pizzo SV. A nonantigenic covalent streptokinase-polyethylene glycol complex with plasminogen activator function. *J Clin Invest*. 1985;75(2):413-419.
12. Kim IS, Choi HG, Choi HS, Kim BK, Kim CK. Prolonged systemic delivery of streptokinase using liposome. *Arch Pharm Res*. 1998;21(3):248-252.
13. Nguyen PD, O'Rear EA, Johnson AE, Patterson E, Whitsett TL, Bhakta R. Accelerated thrombolysis and reperfusion in a canine model of myocardial infarction by liposomal encapsulation of streptokinase. *Circ Res*. 1990;66(3):875-878.
14. Leach JK, Edgar AO, Patterson E, Miao Y, Johnson AE. Accelerated thrombolysis in a rabbit model of carotid artery thrombosis with liposome-encapsulated and microencapsulated streptokinase. *Thromb Haemost*. 2003;90(1):64-70.
15. Chen JP, Liu CH, Hsu HL, Wu T, Lu YJ, Ma YH. Magnetically controlled release of recombinant tissue plasminogen activator from chitosan nanocomposites for targeted thrombolysis. *J Mater Chem B*. 2016;4(15):2578-2590.
16. Chuah LH, Billa N, Roberts CJ, Burley JC, Manickam S. Curcumin-containing chitosan nanoparticles as a potential mucoadhesive delivery system to the colon. *Pharm Dev Technol*. 2013;18(3):591-599.
17. Chuah LH, Roberts CJ, Billa N, Abdullah S, Rosli R, Manickam S. Using Nanoparticle Tracking Analysis (NTA) to decipher mucoadhesion propensity of curcumin-containing chitosan nanoparticles and curcumin release. *J Dispers Sci Technol*. 2014;35(9):1201-1207.
18. Agnihotri SA, Mallikarjuna NN, Aminabhavi TM. Recent advances on chitosan-based micro-and nanoparticles in drug delivery. *J Control Release*. 2004;100(1):5-28.
19. Qi L, Xu Z, Jiang X, Hu C, Zou X. Preparation and antibacterial activity of chitosan nanoparticles. *Carbohydr Res*. 2004;339(16):2693-2700.
20. Lavertu M, Methot S, Tran-Khanh N, Buschmann MD. High efficiency gene transfer using chitosan/DNA nanoparticles with specific combinations of molecular weight and degree of deacetylation. *Biomaterials*. 2006;27(27):4815-4824.

21. Mao HQ, Roy K, Troung-Le VL, et al. Chitosan-DNA nanoparticles as gene carriers: synthesis, characterization and transfection efficiency. *J Control Release*. 2001;70(3):399-421.
22. Mao S, Bakowsky U, Jintapattanakit A, Kissel T. Self-assembled polyelectrolyte nanocomplexes between chitosan derivatives and insulin. *J Pharm Sci*. 2006;95(5):1035-1048.
23. Veilleux D, Nelea M, Biniecki K, Lavertu M, Buschmann MD. Preparation of concentrated chitosan/DNA nanoparticle formulations by lyophilization for gene delivery at clinically relevant dosages. *J Pharm Sci*. 2016;105(1):88-96.
24. Xu Y, Du Y. Effect of molecular structure of chitosan on protein delivery properties of chitosan nanoparticles. *Int J Pharm*. 2003;250(1):215-226.
25. Aeinehvand R, Zahedi P, Kashani-Rahimi S, Fallah-Darrehchi M, Shamsi M. Synthesis of poly (2-hydroxyethyl methacrylate)-based molecularly imprinted polymer nanoparticles containing timolol maleate: morphological, thermal, and drug release along with cell biocompatibility studies. *Polymer Adv Tech*. 2017;28(7):828-841.
26. Hans ML, Lowman AM. Biodegradable nanoparticles for drug delivery and targeting. *Curr Opin Solid State Mater Sci*. 2002;6(4):319-327.
27. Zhang Y, Chan HF, Leong KW. Advanced materials and processing for drug delivery: the past and the future. *Adv Drug Deliv Rev*. 2013;65(1):104-120.
28. Karnik R, Gu F, Basto P, et al. Microfluidic platform for controlled synthesis of polymeric nanoparticles. *Nano Lett*. 2008;8(9):2906-2912.
29. Majedi FS, Hasani-Sadrabadi MM, Emami SH, et al. Microfluidic assisted self-assembly of chitosan based nanoparticles as drug delivery agents. *Lab Chip*. 2013;13(2):204-207.
30. Chen S, Zhang H, Shi X, Wu H, Hanagata N. Microfluidic generation of chitosan/CpG oligodeoxynucleotide nanoparticles with enhanced cellular uptake and immunostimulatory properties. *Lab Chip*. 2014;14(11):1842-1849.
31. Baharifar H, Amani A. Cytotoxicity of chitosan/streptokinase nanoparticles as a function of size: an artificial neural networks study. *Nanomedicine*. 2016;12(1):171-180.
32. Baharifar H, Tavoosidana G, Karimi R, et al. Optimization of self-assembled chitosan/streptokinase nanoparticles and evaluation of their cytotoxicity and thrombolytic activity. *J Nanosci Nanotechnol*. 2015;15(12):10127-10133.
33. Modaresi SMS, Ejtemaei Mehr S, Faramarzi MA, et al. Preparation and characterization of self-assembled chitosan nanoparticles for the sustained delivery of streptokinase: an in vivo study. *Pharm Dev Technol*. 2014;19(5):593-597.
34. Bradford MM. A rapid and sensitive method for the quantitation of microgram quantities of protein utilizing the principle of protein-dye binding. *Anal Biochem*. 1976;72(1-2):248-254.
35. Costa P, Lobo JMS. Modeling and comparison of dissolution profiles. *Eur J Pharm Sci*. 2001;13(2):123-133.
36. Zahedi P, Rezaeian I, Jafari SH, Karami Z. Preparation and release properties of electrospun poly (vinyl alcohol)/poly (ε-caprolactone) hybrid nanofibers: optimization of process parameters via D-optimal design method. *Macromol Res*. 2013;21(6):649-659.
37. Shamsi M, Zahedi P, Ghourchian H, Minaeian S. Microfluidic-aided fabrication of nanoparticles based on chitosan based on a transdermal multidrug application. *Int J Biol Macromol*. 2017;99:433-442.
38. Ratner BD, Hoffman AS, Schoen FJ, Lemons JE. *Biomaterials Science: An Introduction to Materials in Medicine*. 1st ed. San Diego, CA: Academic Press; 1996:497.